Available online at www.sciencedirect.com
ScienceDirect
Journal of Magnetism and Magnetic Materials 320 (2008) 1260–1271
Journal of magnetism and magnetic materials
www.elsevier.com/locate/jmmm

Current perspectives

# Developments in nano-oscillators based upon spin-transfer point-contact devices ☆

T.J. Silva*, W.H. Rippard

*NIST, Electromagnetic Technology Division, Mailcode 814.05, 325 Broadway, Boulder, CO 80303, USA*

Available online 31 December 2007

**Abstract**

We review the current status of research on microwave nano-oscillators that utilize spin transfer devices with point-contact geometry, with an emphasis on the open questions that still prevent our full understanding of device properties. In particular, we examine those aspects that might affect irreproducibility of device performance. While there is a clear picture of the general principles that underlie the properties of the spin torque nano-oscillator, there are a number of details complicating the picture. We suggest that these details are potentially responsible for adversely affecting uniformity of performance from device to device. These details include (1) nonlinearities, (2) the Oersted field, (3) thermal and deterministic noise sources, and (4) non-uniformity of the spin accumulation. We suggest what role that these details might have in determining spin torque dynamics, and suggest particular avenues of investigation that might clarify whether or not these details are indeed responsible for device variability. This article is one of a series devoted to the subject of spin torque in this issue of the *Journal of Magnetism and Magnetic Materials*.
Published by Elsevier B.V.

*Keywords:* Spin torque; Point contact; Nano-oscillator; Nonlinearity; Nonlinear Schroedinger equation; Oersted field; Noise; Chaos; Spin accumulation; Linewidth

## 1. Introduction

The development of spin torque nano-oscillators based upon point-contact geometry [1–4] has opened a wide door of possibilities for nanoscale magnetic devices as active microwave components. For many years, magnetic components have played a key role in microwave technology, primarily in the context of passive devices, such as phase shifters and circulators, where the permeability of the magnetic materials is the key factor for practical applications. The spin torque nano-oscillator, on the other hand, converts a dc electrical current into microwave signals, and, *vice versa*, it can convert a microwave signal into a dc voltage [5]. The introductory article by Ralph and Stiles in this issue of the *Journal of Magnetism and Magnetic Materials* discusses the basic physics that give rise to microwave oscillations in spin torque devices. The microwave linewidth for spin torque nano-oscillators based upon point-contact geometry is in the range of 1–10 MHz, depending on applied current and magnetic field [6]. Signals in the rf range can be even narrower [7]. Nanoscale microwave sources with such narrow linewidth have many potential practical applications. In Fig. 1, we show a typical microwave emission spectrum at 13.2 GHz for a spin torque nano-oscillator that exhibits a linewidth of 7.1 MHz and a peak amplitude of almost 1 mV. The possibility of a narrow-band, nanoscale microwave source and detector has intriguing implications for technological innovation, such as the development of a chip-scale microwave spectrum analyzer. (We refer the reader to the companion article in this issue of the *Journal of Magnetism and Magnetic Materials* by Katine and Fullerton for a more exhaustive discussion of possible applications for spin torque nano-oscillators.) To this end, several efforts are now underway to improve the performance of spin torque nano-oscillators. For example, several groups recently demonstrated methods to eliminate the need for an applied

☆ Contribution of the National Institute of Standards and Technology, an agency of the US Government, not subject to US copyright.

* Corresponding author.
*E-mail address:* silva@boulder.nist.gov (T.J. Silva).

0304-8853/$ - see front matter Published by Elsevier B.V.
doi:10.1016/j.jmmm.2007.12.022

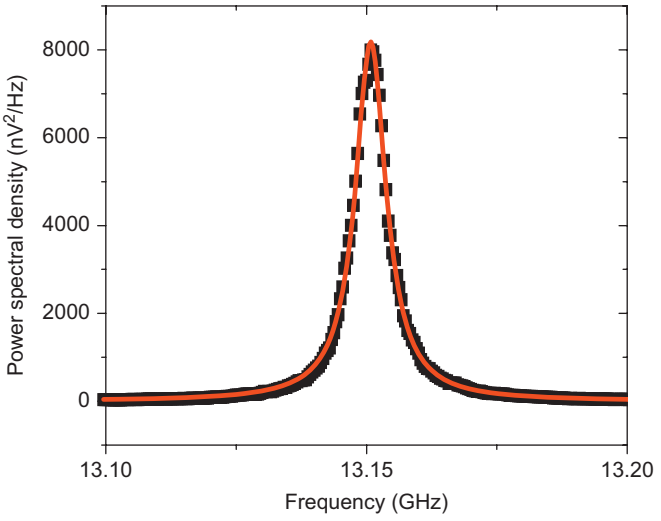


Fig. 1. Spectrum of the emitted microwave signal for a spin torque nano-oscillator using a point contact structure.

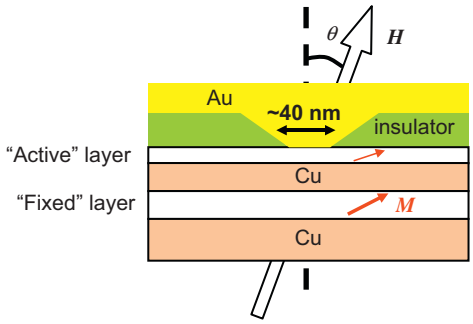


Fig. 2. Cross-sectional sketch of a spin torque nano-oscillator. The two magnetic layers are labeled "active" and "fixed" by virtue of the differing thickness and magnetic moment of the two layers; a thin, low-moment layer has a lower threshold current for excitation of spin-torque-induced dynamics. The trilayer structure below the point contact is of large lateral extent, on the order of tens of micrometers. A magnetic field $H$ is usually applied at some angle $\theta$ when studying gigahertz excitations in such devices.

magnetic field as part of spin torque nano-oscillator operation [8,9]. Other barriers to practical applications for the spin torque nano-oscillator that have yet to be solved include the signal strength and noise performance. However, much is still not understood about the nature of spin torque nano-oscillator operation. Phenomenologically, we understand the essential properties, but we lack quantitatively accurate models for the device performance and the microwave properties. Also, there remains a great deal of variability in device properties, both from lab to lab, and within a single lab. While the former case suggests that the particular fabrication process employed has a strong impact on the physics of spin torque nano-oscillator operation, the latter case equally suggests that the variability of fabrication results at the nanoscale also significantly affects device performance. To improve device repeatability and performance, much work is required to improve our basic understanding of spin torque nano-oscillator operation by systematically examining how the "real-world" details of the spin torque nano-oscillator device alter the essential physics. In other words, it appears that "the devil is in the details" for spin torque nano-oscillator performance. Such details include (1) a broad range of nonlinearities, (2) the Oersted field, (3) thermal and chaotic noise sources, and (4) spatial inhomogeneity of the spin accumulation that drives the spin torque effect. What follows is a brief examination of what is currently known and not known about these four "experimental details" that have yet to be adequately addressed.

First, we provide a brief review of the device structure under discussion. The spin torque nano-oscillator consists of unpatterned magnetic multilayer of the general five-layer pseudo-spin-valve structure, NM/FM/NM/FM/NM, where NM is a non-magnetic conductor, and FM is a magnetic conductor, but with the addition of a nanoscale electrical contact that is made to the upper surface of the multilayer (see Fig. 2). The pseudo-spin-valve is patterned into a large area, rectangular mesa, that is usually tens of micrometers on a side. The ferromagnetic layer closest to the surface with the point contact is generally chosen to be as thin as possible; since the resultant torque that drives the dynamics is actually the difference between the spin torque and the damping torque, reducing the net damping torque by reducing the magnetic volume directly under the electrical point contact improves the efficiency of the device. In other words, the thinner the magnetic layer in question, the less current that is required to overcome the damping torque. Thus, it is usually assumed that the thin layer closest to the contact is the "active" layer, whereas the other, thicker layer, is considered a "fixed" layer that acts as a source of spin accumulation in the non-magnetic conductive spacer between the two FM layers. When dynamics are induced in the active layer, the magnetoresistance of the device becomes time varying, thereby generating a microwave signal. By fabricating appropriate broadband interconnects to the final structure, the resultant microwave signal can be detected and studied.

The microwave signals emitted by point contact structures can vary in frequency from hundreds of MHz to 32 GHz [4]. The frequency of emission is a function of the strength and angle of the applied magnetic field, as well as the dc current. The frequency generally increases with applied magnetic field because the magnetic oscillations are precessional in nature: The larger the net effective magnetic field, the greater the torque acting on the spins, and the higher the frequency of precession. The slope of frequency vs. field is 28 GHz/T when the applied **field is at 40° to the film normal, and roughly18 GHz/T when the applied field is at 10° from the film normal [6]. For a given applied field, the frequency is maximal when the field is applied in the plane of the device [4]. The slope of frequency vs. current can be as high as 1 GHz/mA when the field is applied at 10° from film normal [6]. The physics behind the dependence of frequency on current are discussed later in this article. At present, it is assumed that fields larger than

what have been applied so far will result in even greater frequencies than what have been measured to date, and that the measured maximum frequency is simply limited by the bandwidth of the interconnecting microwave instrumentation. Higher frequency emissions should be detectable through the use of proper cabling and connectors such as 1 mm connectors, which are capable of carrying signals up to 110 GHz.

Low-frequency rf signals with extremely narrow linewidths are observed when a weak magnetic field of less than 4 kA/m (50 Oe) is applied in the film plane [7]. Signals with 10 nW power and linewidths as narrow has 580 kHz have been observed in this geometry. The frequency is a weak function of applied field, with a slope of only 200 MHz/T. The rf oscillations are non-sinusoidal in character, with substantial emissions at higher harmonic frequencies. The mode structure for these low-field modes is believed to originate from the spin-torque-induced oscillations of a vortex-like magnetic structure, which is formed by the Oersted field near the contact [7]. The low frequencies of the microwave emissions, as well as the weak dependence of frequency on field, are characteristic signatures of magnetic vortex resonance [10]. Further discussion of the role of the Oersted field in the dynamics for point contact structures can be found later in this article.

Accompanying the microwave electrical emissions from point contact structures are spin wave emissions in the active magnetic layer [2,11–13]. These co-excited spin waves, which have been predicted by theory [13] and indirectly detected in dual contact experiments [2,11,12], propagate away from the point contact into the surrounding magnetic film. In the dual contact experiments, the radiation of spin waves between two point contacts formed out of the same pseudo-spin-valve structure leads to the phase locking of the two nano-oscillators [2,11]. The ability to lock multiple nano-oscillators using non-electrical means is a unique property of spin torque nano-oscillators based upon point-contact geometry. The structure of the excited spin wave modes is discussed in more detail later in this article.

Microwave emissions are also observed in nanopillars structures, where the active magnetic layer is patterned to the same size as the electrical contact [14–17]. While the frequency range that is accessible to nanopillar nano-oscillators is comparable to that for nanocontacts, it is generally found that the room temperature linewidths for the nanopillars geometry are significantly broader (on the order of hundreds of MHz) [16], though the linewidths are comparable to those of point-contact devices when measured at cryogenic temperatures [15,16]. The possible origin for the larger room temperature linewidth in nanopillars devices is discussed in detail later in this article. However, peaks with linewidths of 10 MHz have been observed in nanopillars devices at room temperature when using dc currents in excess of 3 mA [17]. These narrow linewidth modes are associated with dynamics excited in the thicker fixed layer in the nanopillars structure, which generate significantly weaker microwave signals than modes associated with excitations of the thinner active layer [17]. Low-frequency modes associated with the vortex core resonance in the thick fixed layer have also been observed in nanopillars [9].

## 2. Nonlinearities

Until the last decade, the study of nonlinear dynamics in ferromagnetic systems was centered primarily on the microwave-pumped response in micrometer-thick yttrium iron garnet (YIG) films. Several reasons account for this concentration of effort on the part of the nonlinear dynamics community. First, the nonlinear properties of ferromagnetic materials at microwave frequencies are dominated by the coupling between the uniform ferromagnetic resonance (also known as "the FMR mode") and the spinwaves at either a degenerate frequency (the "second-order" or "four-magnon" process) or half of the FMR mode frequency (the "first-order" or "three-magnon" process) [18]. This coupling, which is sometimes referred to as "the Suhl instability", limits the power absorbed by a ferromagnet when pumped at the FMR mode; at sufficiently high power, well below the geometrical saturation point (i.e., the excitation level at which the effective longitudinal component of the magnetization is zero), all additional pump power is diverted into the production of degenerate frequency spin waves [19]. This premature saturation effect effectively limits the excitation amplitudes to a level that is one to two orders of magnitude below the saturation point [20]. Second, the pump power at which such nonlinear effects occur is proportional to the intrinsic damping of the material. Since YIG has the lowest damping of any known ferromagnet ($\alpha \approx 0.0001$), it is a natural choice for such nonlinear studies (though the effect has been observed in metallic films.) Finally, the existence of nonlinearly coupled spin wave modes necessarily requires substantial film thickness such that there is a large density of states for magnetostatic backward volume wave (MSBVW) modes. (The MSBVW modes have a wavevector that is parallel to the average magnetization direction. Due to dipole field effects, the group velocity for the MSBVW is negative at low wavenumbers [21].) In other words, for somewhat complicated reasons that go beyond the scope of this paper, the in-plane component of the dipole–dipole coupling fields must be sufficiently large to give rise to degenerate and half-frequency magnon modes. Given all of these technical reasons, substantial effort has gone into the study and application of nonlinear dynamics in thick YIG films [22]. This state of affairs changed substantially with the advent of the spin torque nano-oscillator.

With the spin torque nano-oscillator, a high current density injected into an unpatterned thin-film structure through a lithographically defined point contact gives rise to spatially non-uniform precessional oscillations of the

magnetization that can have very large amplitudes, approaching geometrical saturation. While the details of the excitation distribution in the active magnetic layer(s) are still the subject of intense study, most researchers generally believe that the excitations are a maximum directly under the point contact, and that spin waves of some form may or may not propagate away from the contact region, depending on the details of the spin wave band structure, the nonlinear dependence of the excitation frequency on excitation amplitude, and the equilibrium magnetization direction. In Fig. 3, we show micromagnetic simulation results that display isotropic spin wave generation in the case of a point contact structure with a saturating magnetic field applied perpendicular to the film plane. (The Oersted field, to be discussed later in this article, has been ignored for this particular calculation.) The formation of such magnetic excitations in such a device can be understood in terms of the negative "effective" damping that spin torque gives rise to; once the current density directly under the point contact is sufficiently large, the total effective damping (intrinsic damping plus radiative spin wave damping plus spin torque) in some finite region of the active material is zero, precessional oscillations of the magnetization spontaneously arise as a result of the induced instability. As mentioned earlier in this article, the oscillations are measured via the giant magnetoresistance dependence of the voltage across the device on the relative orientation of the magnetization in the two ferromagnetic layers: when the magnetization between the two layers is parallel, resistance is minimum, and when it is antiparallel, the resistance is maximum. Between these two extremes, the resistance follows a cosine dependence on relative angle of the magnetization in the two layers. Depending on the current density, the amplitude of these magnetic oscillations can be quite large, even approaching geometrical saturation. Thus, a variety of nonlinear phenomena are both predicted and observed in the case of the spin torque nano-oscillator.

Fig. 3. Micromagnetic simulation snap-shot of steady-state spin wave generation in a point-contact geometry. The image portrays a region of the active magnetic layer of 2.4-μm diameter at a particular instant in time. The contact is 80 nm in diameter, located at the center of the displayed disk. A saturating magnetic field is applied perpendicular to the film plane. The amplitude is proportional to one of the in-plane components of magnetization. The resultant spin waves have a frequency of 4.4 GHz (courtesy of Mark Hoefer).

Slonczewski [13] provided the first calculations of the threshold current for spin wave generation in a point-contact geometry. We start with the Landau–Lifshitz equation and include the Slonczewski torque term:

$$\frac{\partial \vec{M}}{\partial t} = -|\gamma|\mu_0\left(\vec{M}\times\left(\vec{H}_{\text{eff}}+\frac{\alpha}{M_s}(\vec{M}\times\vec{H}_{\text{eff}})\right)\right) + \beta\vec{M}\times(\vec{M}\times\hat{m}_{\text{fix}}), \quad (1)$$

where $\gamma$ is the gyromagnetic ratio, $\mu_0$ is the permeability of free space, $\alpha$ is the dimensionless Landau–Lifshitz damping parameter, $M_s$ is the saturation magnetization, $\beta$ is the spin torque coefficient, $\hat{m}_{\text{fix}}$ is a unit vector pointing in the direction of the "fixed" layer magnetization, and the effective field $\vec{H}_{\text{eff}}$ is given by

$$\vec{H}_{\text{eff}} \doteq \vec{H}_0 - M_z\hat{z} + \frac{D}{\gamma\hbar\mu_0 M_s}\nabla^2\vec{M}, \quad (2)$$

where $D$ is the exchange parameter (typically on the order of $6.4\times10^{-37}\,\text{J m}^2$, or $4\,\text{meV nm}^2$). We are ignoring crystalline, surface, or any other induced anisotropy because the active magnetic layer is usually formed from a magnetically soft polycrystalline alloy. We are also ignoring any non-local in-plane component of the dipole fields due to gradients of the in-plane magnetization. It has been shown that the in-plane dipole fields are relatively insignificant when the active magnetic layer is on the order of 5 nm or thinner [23].

In Eq. (1), the spin torque coefficient $\beta$ is given by

$$\beta \doteq \frac{J\hbar\gamma\varepsilon}{2M_s^2\delta e}\theta(r_* - r), \quad (3)$$

where $J$ is the current density, $\hbar$ is Planck's constant divided by $2\pi$, $\varepsilon$ is the spin torque efficiency (with $0<\varepsilon<1$), $\delta$ is the free layer thickness, $e$ is the electron charge, $\theta(r_*-r)$ is the Heaviside step function, and $r_*$ is the contact radius. We then consider the high-symmetry case with an applied magnetic field that saturates the magnetization in a surface normal direction. Given the high symmetry of the geometry, radial units may be employed, and we obtain the following linear approximation of the Landau–Lifshitz equation in dimensionless form:

$$\mathrm{i}\frac{\partial m}{\partial \tau} \cong (\tilde{\nabla}^2 - (h-1))m + \mathrm{i}(\alpha(\tilde{\nabla}^2 - (h-1)) + j\theta)m, \quad (4)$$

with the normalizations

$$m \doteq (M_x/M_s) + \mathrm{i}(M_y/M_s), \quad h \doteq H/M_s,$$
$$\tilde{\nabla}^2 \doteq \frac{1}{\rho}\frac{\partial}{\partial\rho}\left(\rho\frac{\partial}{\partial\rho}\right), \quad \rho \doteq r/\ell_{\text{ex}},$$
$$\ell_{\text{ex}} \doteq \sqrt{D/\hbar\omega_M}, \quad \omega_M \doteq \gamma\mu_0 M_s,$$
$$\tau \doteq \omega_M t, \quad \text{and} \quad j \doteq [(\hbar\varepsilon)/(2M_s^2 e\mu_0\delta)]J.$$

In this simplified form, we readily see that Eq. (4) is very similar to the Schrödinger equation, but with an additional imaginary term due to damping and spin torque.

If we assume a steady state, standing wave solution within the contact of the form $m(r,t)=\tilde{m}(r)e^{-i\omega t}$, then the second term in Eq. (4) results in a complex frequency $\omega$, i.e., the mode either grows or decays exponentially with time. In the absence of current, $\mathrm{Im}(\omega)<0$, and the solution decays with time. At a critical current density $j_{\mathrm{crit}}$ such that $\mathrm{Im}(\omega)=0$ for $r<r_*$, a stable linear solution exists. The linear mode stability criterion is therefore

$$j_{\mathrm{crit}}=\left(-\left\{\alpha\,\mathrm{Re}\left(\frac{\tilde{\nabla}^2 m}{m}\right)+\mathrm{Im}\left(\frac{\tilde{\nabla}^2 m}{m}\right)\right\}+\alpha(h-1)\right),\quad \text{for } r<r_*. \tag{5}$$

Slonczewski solved Eq. (4), assuming a stable solution, in terms of Bessel and Hankel functions, resulting in eigenvalues for the critical current and the onset frequency in the limit of $\alpha\to 0$. (The eigenvalues are derived by matching the solution and its derivative at the contact radius.) From his result, we obtain $\mathrm{Im}(\tilde{\nabla}^2 m/m)\approx -1.86/\rho_*^2$, and $\mathrm{Re}(\tilde{\nabla}^2 m/m)\approx -1.43/\rho_*^2$, to the zeroth order in $\alpha$. Substituting these two approximations for the real and imaginary parts of the Laplacian back into Eq. (5), we obtain the following approximate critical current for the threshold of spin wave generation:

$$j_{\mathrm{crit}}=\left(\frac{1.86}{\rho_*^2}+\alpha(h-1+h_{\mathrm{ex}})\right), \tag{6}$$

where $h_{\mathrm{ex}}=1.43/\rho_*^2$ is the exchange field associated with the excited spin wave mode. The first term in Eq. (6) describes the effective damping torque due to spin wave radiation away from the contact. The second term describes the intrinsic damping torque. For typical experimental parameters ($\alpha\approx 0.01$, $1<h<2$, $r_*\approx 20$ nm, $\ell_{\mathrm{ex}}\approx 6$ nm), we find that $\rho_*^2\alpha(h-1)\approx 0.1$, such that Eq. (6) is to a good approximation simply $j_{\mathrm{crit}}\approx 1.86/\rho_*^2$; the critical current is determined primarily by the loss associated with spin wave radiation away from the point contact, and depends only weakly on the intrinsic damping. This is to be contrasted with the case of nanopillar excitations, where spin wave radiation does not affect the critical current threshold. Once the critical current is exceeded in the case of nanocontacts, stabilization of the spin wave amplitude to a finite value occurs as a result of nonlinearities, as we shall now describe.

First and foremost, the nonlinearity of the spin torque nano-oscillator is manifested most obviously by the dependence of the oscillation frequency on the injected current level. Both red-shifting ($df/dI<0$) and blue-shifting ($df/dI>0$) behaviors have been observed [4]. Such nonlinearity can be coarsely understood in terms of the dependence of the FMR stiffness fields on the excitation amplitude. For example, if the magnetization in equilibrium (zero current) is pointing perpendicular to the plane of the device owing to the application of a substantial perpendicular magnetic field, the local demagnetizing field will decrease with increasing excitation amplitude. This in turn results in an increase in the total magnetic field (applied field plus demagnetizing field,) thereby driving up the precession frequency. Such behavior has indeed been observed experimentally with point-contact devices in the perpendicular geometry, as shown in Fig. 4, where we present previously published data for the current dependence of the frequency for the emitted microwave signals.

Here, we see that the situation giving rise to nonlinear dynamics via spin torque is inherently different from that observed in the case of FMR. In particular, energy from the exciting current is coupled directly to spin waves via the non-uniformity of the excitation current (and, thereby, the concentration of the spin accumulation near the contact). However, the nature of the excited spin wave modes and their dependence on the experimental parameters, including applied field strength, applied field angle, current magnitude, contact size, and the magnetic moment density of the active layer remains largely unknown. Particularly lacking is any information concerning the spatial distribution of the excited spin wave modes. While there is experimental evidence that spin waves are indeed generated, and that the excited spin waves can even act as a means for the coupling of contiguous spin torque nano-oscillators in a shared trilayer structure [2,11,24], we do not know how the spin wave radiation from a given contact is spatially distributed. Nor do we know how the spin wave modes propagate when their amplitude is in the strongly nonlinear regime, or even whether stable modes exist in this regime. While it has been predicted that the excited spin waves are localized about the point contact in the case of a red-shifting nonlinearity (so-called localized spin wave "bullet") [25], these predictions have not yet been directly

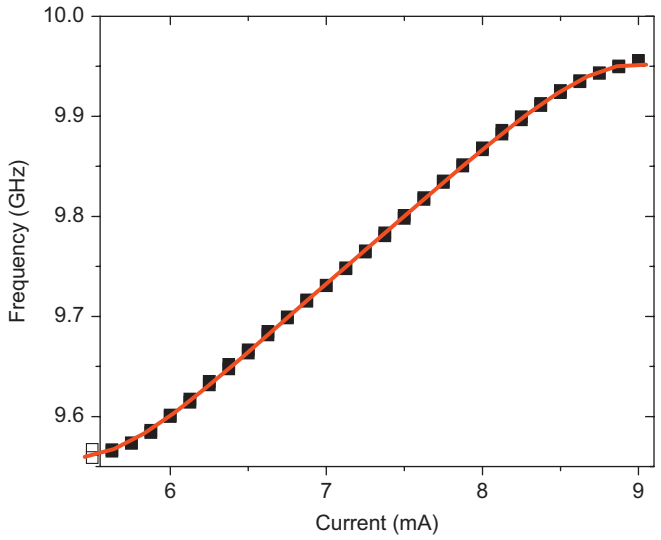


Fig. 4. Frequency vs. current for spin torque nano-oscillator, where the applied field is tilted a few degrees away from the normal to the film. The frequency increases with increasing current as a result of nonlinearity inherent in the magnetization dynamics of large amplitude in a thin-film geometry.

confirmed. Even here, there are clear distinctions with the nonlinearities associated with high-power FMR of micrometer-thick YIG films; the active layers in the spin torque nano-oscillator structure are generally less than 5 nm thick, precluding the existence of a significant density of MSBVW modes. Instead, the resultant nonlinearities are due predominantly to the local dipole–dipole interactions (i.e., the demagnetizing field) and the exchange interaction. The latter case is worth elaborating further.

Consider the case where a magnetic field $H$ is applied perpendicular to the film plane of a magnitude sufficient to saturate the magnetization in the film normal direction. If we expand the Landau–Lifshitz equation (including the Slonczewski torque term) to second order in excitation magnitude $|m|$, we obtain a complex Ginzberg–Landau equation [26]:

$$\begin{aligned} \mathrm{i}\frac{\partial m}{\partial \tau} = {} & \{(\tilde{\nabla}^2 - (h-1)) + \mathrm{i}(\alpha(\tilde{\nabla}^2 - (h-1)) + j\theta) \\ & + \frac{1}{2}[-|m|^2 - \mathrm{i}(j\theta - \alpha(h-2))|m|^2 \\ & + (m\tilde{\nabla}^2 m^* + 2(1+\mathrm{i}\alpha)|\tilde{\nabla}m|^2)]\}m. \end{aligned} \tag{7}$$

While Eq. (7) appears complicated, we can identify the role of the primary nonlinearities by considering the case of zero spin torque and zero damping. In this case, Eq. (7) simplifies to

$$\begin{aligned} \mathrm{i}\frac{\partial m}{\partial \tau} = {} & \left\{(\tilde{\nabla}^2 - (h-1)) - \frac{1}{2}|m|^2 \right. \\ & \left. + \frac{1}{2}(m\tilde{\nabla}^2 m^* + 2|\tilde{\nabla}m|^2)\right\}m. \end{aligned} \tag{8}$$

The last two terms within the curly brackets on the right-hand side of Eq. (8) are nonlinear corrections for the exchange interaction. We should note that the appearance of such a nonlinearity in the case of the complex Ginzberg–Landau equation is highly unusual; such terms do not appear in the usual derivation of the Ginzberg–Landau equation when using the slowly varying envelope approximation under conditions of weak nonlinearity, as is usually done in nonlinear optics [27].

Let us assume, in a slowly varying envelope approximation, that $m$ has the approximate form $\tilde{m}\exp(i\kappa\rho)\exp(i\Omega\tau)$ for $\rho \gg 1$, where $\kappa \doteq k\ell_{\mathrm{ex}}$, $\Omega$ is the normalized mode frequency, and $\tilde{m}$ is the slowly varying envelope function with a characteristic length scale much greater than $1/k$. Substituting our assumed solution into Eq. (2) and dividing out common factors, we obtain the nonlinear dispersion relation:

$$\Omega \cong \kappa^2 + (h-1) + \tfrac{1}{2}a^2 - \tfrac{1}{2}a^2\kappa^2, \tag{9}$$

where $a \doteq |m|$. The first term in Eq. (9) is due to linear exchange, the second is due to the net internal magnetic field (applied field plus demagnetizing field), the third is due to the nonlinearity of the demagnetizing field, and the last is due to nonlinear exchange. If we ignored the nonlinearity due to exchange, our nonlinear dispersion relation would be that for the nonlinear Schrödinger equation (NLSE) [28]. A well-known result for NLSE is that, if $\mathrm{d}\kappa/\mathrm{d}a > 0$ for a constant $\Omega$, a localized "soliton" solution is possible: the so-called "Lighthill criterion." [29] When the Lighthill criterion is satisfied, the larger the amplitude of the envelope function, the shorter the wavelength of the sinusoidal component. Also, when the amplitude falls below a threshold value, the wavenumber becomes imaginary; the wavepacket has evanescent tails that bound the wavepacket. For the present case, in the absence of the exchange nonlinearity, the last term in Eq. (9) (i.e., the term that gives rise to a blue shift in frequency with increasing amplitude) is of the wrong sign to support a soliton solution. However, if we account for nonlinear exchange, solving for $\kappa$ in terms of $a$ in Eq. (9), we find that $\mathrm{d}\kappa/\mathrm{d}a > 0$ is possible, but only for $\Omega > 1$. As to whether this is a sufficient condition for exchange-induced localization is not entirely clear, but the possibility that such a novel localized nonlinear "exchange" wave solution exists at high frequencies in magnetic nanostructures certainly warrants further investigation.

Tiberkevich and Slavin [30] recently proposed that the Gilbert damping should also manifest a nonlinearity in the limit of large excitation amplitudes. The proposed nonlinear Gilbert damping takes the form

$$\alpha = \alpha_{\mathrm{G}}\left(1 + q_1\frac{\left|\partial\vec{M}/\partial t\right|^2}{\omega_M^2 M_0^2}\right), \tag{10}$$

where $q_1$ is the phenomenological nonlinear damping coefficient on the order of unity. Introducing such a nonlinearity is necessary in order to fit spin-transfer-induced oscillation data for a nanopillar structure when using a macrospin-based theory including dipole-induced nonlinearity. It is argued that such nonlinearity is a reasonable expectation for any physical damping mechanism, but there exists no *ab initio* theory for such nonlinearity. We should emphasize that the nonlinearity expressed in Eq. (10) is in practice a very subtle effect. In the case of conventional FMR with a soft NiFe alloy ($Ni_{80}Fe_{20}$), we can estimate that the increase in damping due to the proposed nonlinearity is only 0.5% for a large pump field of 480 A/m (6 Oe) at 9 GHz (80 kA/m applied field), at which the excitation amplitude is approximately 20% of geometrical saturation, equivalent to 12° of angular rotation. (This assumes that the Suhl instability is ineffective, as is the case when one is measuring a very thin film of less than 10 nm.)

Kambersky and Patton [31] have developed a comprehensive theory for magnon–electron damping in metals, which was recently expanded on to be fully quantitative for the transition metals (Fe, Ni, and Co) [32]. The magnon-electron theory is exciting because it correctly predicts both the magnitude *and* the temperature dependence of the damping for the transition elements. However, the nonlinear extension of magnon–electron theory in the limit of large amplitude excitations has not been done. In either

case, nonlinear modification of the Gilbert damping coefficient should have little effect on spin torque nano-oscillator operation as long as the excited mode structure takes the form of radiating spin waves, because the energy loss from the contact region due to spin wave radiation dominates the intrinsic Gilbert losses. If, however, the excited mode is localized, the role of the Gilbert damping, including any nonlinearity, becomes important. This is seen, for example, in the numerical simulation results of Consolo et al. [33] where the critical current for a localized bullet mode increased by more than a factor of two when nonlinear damping was included in the calculation, whereas the critical current for the so-called "linear" mode was hardly affected.

## 3. The Oersted field

Compounding the complexity of the spin torque nano-oscillator problem is the question of the Oersted fields produced by the current flow. For a wire of a 20 nm radius carrying 10 mA of current, the Oersted field is $\approx$80 kA/m (1000 Oe) at the surface of the wire. While the current flow in the point-contact geometry is not exactly that for a wire of infinite extent, the infinite wire approximation happens to provide a reasonable order of magnitude estimate [23]. Thus, the Oersted field is clearly not a minor perturbation in this problem. How the Oersted field exactly affects the dynamics remains an open question. In the case where a saturating magnetic field is applied perpendicularly to the device plane, the Oersted field clearly establishes a static vortex magnetization pattern. When spin torque is taken into account, we expect a mode with helical symmetry, i.e., the phase of the magnetization precession changes by 180° when reflecting about a point at the center of the point contact. However, micromagnetic simulations [34], using the NIST micromagnetic code OOMMF [35], show that this vortex wave is unstable in the presence of any symmetry-breaking perturbations, such as the slight misalignment of the applied field from perfectly normal to the device plane or the corrugation of the simulated system by the Cartesian finite element grid. This example highlights the need to treat all analytical models for the spin torque nano-oscillator skeptically, especially when the models require a high degree of symmetry to make the problem tractable. Incorporation of the many experimental details that reduce the symmetry of the problem appears to be a necessary step in formulating an accurate model of magnetization dynamics in spin torque nano-oscillators.

We already have some idea how the Oersted field can substantially impact dynamics in point-contact geometry. For example, as previously described in the Introduction, the Oersted field can nucleate a vortex structure in a continuous film where the vortex core undergoes rf oscillations due to spin torque in weak applied in-plane field [7]. Unfortunately, micromagnetic simulations are not yet able to properly model such vortex core dynamics in an unrestricted film given the numerical restrictions on the size of the modeled domain.

When sufficient magnetic field is applied in the film plane to exceed the Oersted field at the edge of the contact, the superposition of the Oersted field and the applied field results in a spatially varying local magnetic field with a sharp minimum in magnitude at the edge of the contact where the Oersted field is opposed to the in-plane field. A vector field map is shown in Fig. 5 for just such a case, where the contact size is 40 nm in diameter, the in-plane applied field in the $+x$ direction is 27 kA/m (900 Oe), and the current flowing through the contact is 7.75 mA. Under these conditions, the $x$-component of the magnetic field is positive everywhere in the film plane, precluding formation of a magnetic vortex. Note the clear field minimum at (0, 20 nm) and maximum at (0, −20 nm). We expect that such an inhomogeneous field distribution, while lacking in the symmetry necessary to form a vortex, will nevertheless severely impact the magnetization dynamics induced by spin torque for such a geometry. For example, it is possible that such a minimum in the spatial field distribution could give rise to a localized excitation mode in much the same manner that the superposition of a transverse applied field and the demagnetizing field at the edge of a magnetic strip gives rise to a localized edge mode [36]. This would be a purely linear mechanism for localization of spin-torque-induced excitations, in contrast to the nonlinear process proposed by Slavin and Tiberkevich [25]. Whether such a localized Oersted mode can be excited by spin torque in a pseudo-spin-valve configuration is not yet clear.

The Oersted field plays a less important role in nanopillars spin torque nano-oscillators [15]. This is to be expected because the demagnetizing fields at the edges of

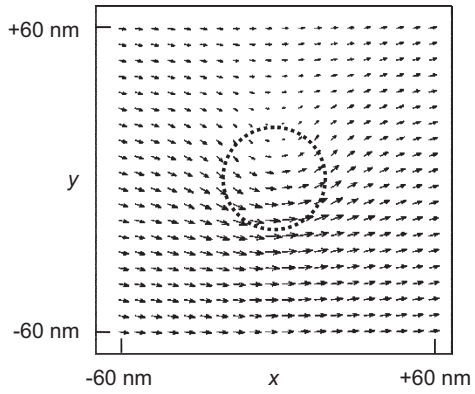


Fig. 5. Vector field map of magnetic field in proximity to a point contact, including both the Oersted field and an in-plane applied field of 72 kA/m (900 Oe). The point contact diameter of 40 nm is indicated with the dotted line. A current of 7.75 mA is flowing through the contact, perpendicular to the film surface. We have approximated the Oersted field as that for an infinitely long wire. While the $x$-component of the net magnetic field is non-zero and positive everywhere in the film plane, thus precluding the formation of a magnetic vortex, there is still a sharp field minimum, as well as a maximum, at the edges of the contact. Exactly how the presence of such spatially localized extrema affects the dynamics induced via spin torque is not yet understood.

the nanopillars have a far greater influence than the Oersted field on the internal field distribution in a nanomagnet.

## 4. Noise sources

The effects of thermal fluctuations on the performance of spin torque nano-oscillators are currently a subject of both theoretical and experimental investigation. Thermal fluctuations are a possible candidate to explain the linewidths measured in all spin-torque-based oscillators, whether they are based on nanocontacts or nanopillars. Kim et al. [37] using a macrospin approximation for the dynamics in the spin torque nano-oscillator, have derived the following equation for the linewidth:

$$\Delta\omega = \Gamma_0\left(\frac{k_B T}{E_0}\right)\left[1+\left(\frac{N}{\Gamma_{\text{eff}}}\right)^2\right], \tag{11}$$

where $\Gamma_0$ is the damping expressed in frequency linewidth, $N \doteq \mathrm{d}\omega/\mathrm{d}A$ is the nonlinear frequency shift ($A \doteq (M_s - M_z)/2M_s$), $E_0$ is the average oscillator energy, and $\Gamma_{\text{eff}}$ is an effective damping that takes into account nonlinearities in both the positive Gilbert-like damping and the "negative" damping induced by the spin torque [37]. The appeal of Eq. (11) rests in part on the simple intuition that thermal fluctuations of the magnetization while precessing causes both phase noise and amplitude noise, the latter being converted to some extent into additional phase noise due to the nonlinear frequency shift (i.e., the last two terms in Eq. (9)). However, the appropriate evaluation of $E_0$ would seem to be an important part of the problem. Kim et al. [37,38] argue that a reasonable approximation for $E_0$ is simply $E_0 = (\omega/\gamma)M_s V_{\text{eff}}$, where

$$V_{\text{eff}} = (E_{\text{tot}}/E_{\text{loc}})\pi r_*^2 \delta. \tag{12}$$

In Eq. (12), $E_{\text{tot}}$ is the total energy of the excited spin wave mode (or modes), $E_{\text{loc}}$ is the energy of the spin wave modes immediately under the point contact, $r_*$ is the contact radius, and $\delta$ is the active magnetic layer thickness. In other words, the effective mode volume scales with the ratio of total magnetic energy to that fraction of energy located immediately under the contact. The claim is made in Ref. [37] that this explains the striking discrepancy in linewidth between the point contact spin torque nano-oscillator when an unpatterned trilayer structure is used, and the room-temperature linewidth obtained with nanopillars structures, which are typically two to three orders of magnitude broader [37].

Why this fraction $E_{\text{tot}}/E_{\text{loc}}$ determines the effective mode volume is not yet clear, nor is it clear whether Eq. (12) is a general result for any given mode distribution, or whether it pertains only to the case of isotropically radiating spin waves. In particular, since Eq. (11) was derived using a macrospin approximation, it appears that the validity of Eq. (11) for the case of extended modes (i.e. spin waves in an extended medium) has not yet been clearly demonstrated. What is clear is that Eqs. (11) and (12) actually imply that linewidth for the spin torque nano-oscillator oscillations should scale *quadratically* with the intrinsic damping if non-localized spin waves are generated, since the effective mode volume (i.e., $E_{\text{tot}}$) for a radiating spin wave will also scale in inverse proportion to the damping constant of the material in question. (Because the characteristic decay length for excited spin waves propagating into the surrounding magnetic medium scales as $1/\alpha$, the effective mode volume, and therefore the total mode energy $E_{\text{tot}}$, is also proportional to $1/\alpha$.) Thus, we might expect that incorporation of low damping materials into spin torque nano-oscillators might greatly improve the noise performance. On the other hand, if Eqs. (11) and (12) are a general result, the implication is that the noise performance should also depend strongly on the mode structure. For example, if the mode is a spin wave "bullet", we would expect the noise performance to be particularly poor since the mode energy would be localized under the point contact. Then there is the inverse dependence on the power of the excitation; for a given mode volume, the oscillation linewidth should scale inversely with the squared amplitude. A clear demonstration of this prediction is still needed.

However, all noise predictions based upon Eqs. (11) and (12) warrant some skepticism, given the nature of the approximations and/or assumptions used in deriving Eq. (11) (i.e., the macrospin approximation that ignores any propagation/retardation effects in the problem) and Eq. (12) (i.e., the assumption that thermal noise for a freely propagating mode in a lossy medium is uniformly distributed over the volume that the mode occupies). A more general theory that naturally includes spatial non-uniformity of the magnetization (as opposed to an *ad hoc* calculation of effective mode volume) seems to be required. However, a micromagnetic approach to the linewidth problem is probably beyond the capability of even the latest computation tools; given that experimentally measured linewidths are on the order of 1–10 MHz [1], simulation periods as long as 1 μs are required to obtain sufficient statistics for an accurate estimation of linewidth. Assuming a simulation time step of 1 ps [39], such a calculation requires as many as $10^6$ time steps, and if each time step requires only 1 s of actual computation time (probably a gross underestimate), such a simulation would run as long as 280 h for a single data point!

The experimental picture with regard to linewidth supports the notion that the situation is far more complicated than any present simple theory would suggest. For example, Rippard et al. [6] found that linewidth varies significantly with changing applied field strength, applied field angle, and applied current, as shown in Fig. 6. In general, it was found that the narrowest linewidths were obtained at an applied field angle of 10° (relative to the film normal) and moderate applied fields of 0.6–0.9 T, though there are regions in the parameter space of current and field strength where the linewidth broadens significantly to

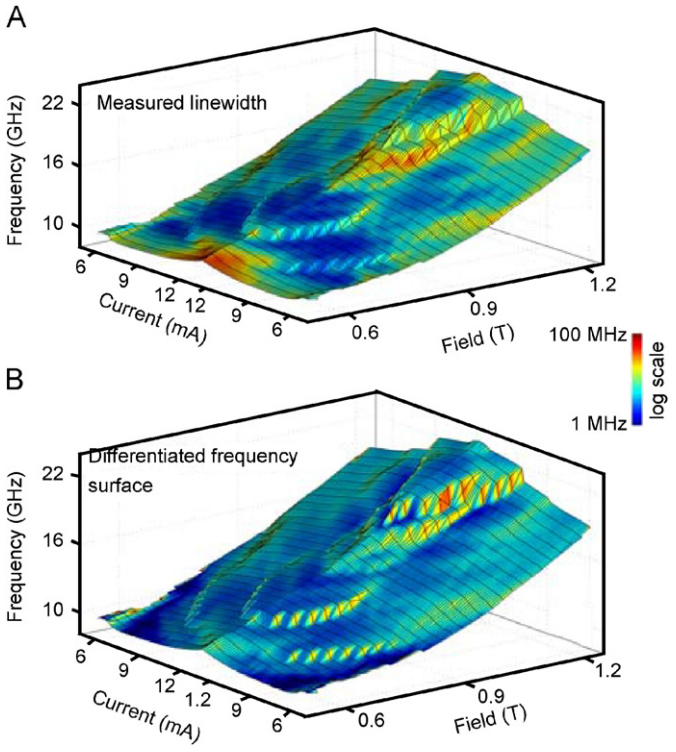


Fig. 6. Experimental point contact data from Ref. [6] showing the dependence of frequency, measured linewidth in (A), and predicted linewidth in (B) on current and applied magnetic field strength for an applied field angle of 10° from surface normal. The linewidth prediction in (B) assumes that the linewidth was the result of uncorrelated fluctuations in field and current, with rms values of 0.8 kA/m (10 Oe) and 1 μA, respectively. The prediction is in reasonable agreement over much of the data, especially where the frequency gradients in field and current are at local maxima. Used with permission of the authors.

values in excess of 100 MHz [6]. The details of why this is the case are not yet clear, though it was found that larger linewidths are correlated with portions of parameter space where the variation of frequency with current and/or field is particularly large. In particular, it is found that the frequency jumps discontinuously along well-defined lines in parameter space, and that the linewidth is significantly enhanced along these lines of discontinuous frequency. A similar result was obtained for nanopillars [15]. This suggests that a variety of modes can be simultaneously excited in point contact structures, and that competition between modes can be another source of linewidth and noise.

Kim et al. [37] explain the minimum average linewidths at 10° by resorting to Eq. (11). The nonlinear frequency shift $N$ undergoes a sign change for sufficiently large applied fields at approximately 10°. For smaller angles, the frequency shift is positive (i.e., the frequency increases with increasing current) and for larger angles, the frequency shift is negative. The reason for the positive frequency shift at small angles is discussed earlier in this article. The negative frequency shift at larger applied field angles, as succinctly explained by Krivorotov et al. [15] is understood in terms of highly elliptical precessional motion, which occurs when a significant component of the time averaged magnetization lies in the film plane; for such highly elliptical orbits, the rate of magnetization change $\mathrm{d}|\vec{M}|/\mathrm{d}t$ is a relatively weak function of oscillation amplitude, whereas the orbital path length is a stronger function of increasing amplitude. The net effect is for the precession frequency to necessarily decrease with increasing amplitude of motion. Thus, for a sufficiently large applied field, there is an applied field angle where the nonlinear frequency shift is zero, thereby minimizing Eq. (11). However, we should point out that the linewidth vs. field angle data presented in Fig. 6A, in Ref [6] is the *average linewidth* obtained over a large range of dc currents and applied field magnitudes, whereas the values calculated by Kim et al. are for specific values of field (0.9 T) and current (9 mA) [37]. While the smallest *average* linewidths were indeed experimentally observed for a field angle of 10°, this does not imply that the nonlinear frequency shift is negligible at this angle *for all values of field and current*. Indeed, there are positions in the $(H,I)$ plane shown in Fig. 6 where $\mathrm{d}f/\mathrm{d}I$ exceeds 1 GHz/mA.

Another issue to consider is the fact that many sources of broken symmetry are associated with a realistic spin torque nano-oscillator. The Oersted field breaks the isotropic azimuthal symmetry. The application of a canted magnetic field breaks the orientation symmetry of the sample plane. Any defect in the magnetic layer breaks the radial symmetry. Thus, it becomes apparent that the magnetization dynamics operate in a space with many degrees of freedom, as opposed to the two degrees of freedom usually considered in conventional FMR or for a macrospin model. When we then include both dipolar and exchange nonlinearities in the problem, we begin to question whether the magnetic trajectory of the precessional excitation necessarily forms a closed, steady-state orbit. Indeed, micromagnetic simulations suggest [16,34] that the orbits have qualities akin to "attractors" in chaos theory [40]. That is to say, the orbits are not quite periodic. (By "periodic" we mean that all degrees of freedom return to a well-defined initial state after some finite duration.) Instead, we observe that the orbits tend to occupy a particular volume in phase space, and that the orbit appears to suffer from some degree of purely deterministic "noise." Given the large number of numerical degrees of freedom for such micromagnetic simulation, with thousands of finite element cells, and given the types of nonlinearities that affect the dynamics, such a tendency towards something like chaos in spin torque nano-oscillator dynamics would not be surprising. If such micromagnetic simulations are accurate (which is itself an ongoing subject of debate), the linewidth of the spin torque nano-oscillator microwave emissions may not be strictly a function of thermal fluctuations, but may also have properties that reflect the dimensionality of chaotic motion about an attractor. Put another way, we may usually assume that thermal fluctuations for a classical periodic oscillator "knocks" the system away from the steady-state

orbit toward which the system then relaxes at a rate given by the intrinsic damping of the system. If a steady-state orbit does not actually exist, and the system is evolving instead in proximity to an attractor in phase space, then thermal fluctuations would tend to either simply modulate the chaotic motion already inherent in the system, or drive the system from one attractor to another. Clearly, to address this question on a theoretical level, more accurate models for spin torque nano-oscillator dynamics are required.

Sankey et al. [16] have measured the temperature dependence of linewidth for microwave emissions from nanopillars devices. Instead of the linear temperature dependence predicted by Kim et al. [37], the linewidth decreases supralinearly with decreasing temperature at high temperatures ($T > 100$ K), and apparently plateaus at low temperatures ($T < 100$ K). (Sankey et al. [16] modeled the low-temperature behavior as scaling with $T^{1/2}$, based upon their own Landau–Lifshitz macrospin model for temperature-dependent linewidth.) Although nanopillar devices differ substantially from the spin torque nano-oscillator based upon point-contact geometry, a linear dependence of linewidth on temperature has so far not been experimentally observed, once again supporting our conclusion that the simplifying assumptions associated with calculations of temperature-dependent linewidth may need revision. On the experimental side, more data are required by use of a substantial number of devices before any conclusions can be reached about the phenomenological behavior of linewidth vs. temperature.

## 5. Non-uniform spin accumulation

The spatial non-uniformity of the excited mode affects frequency and noise performance in a variety of ways. For example, if the magnetization distribution is non-uniform, the spin accumulation in the non-magnetic contacts is also non-uniform. Any non-uniformity in the spin accumulation necessarily means that there are additional gradients in the spin current transverse to the magnet/non-magnet (FM/NM) interface, which, in turn, means that additional sources of torque are acting on the magnetic layer. The theory for such a "transverse spin diffusion" source of spin torque has been elaborated on by numerous authors [41–45], and limited experimental confirmations have been obtained via measurements of differential resistance in single layer structures [46].

One approach to the transverse spin diffusion problem is to separate the longitudinal and transverse components of the spin accumulation, where the longitudinal component is parallel to the axis defined by the equilibrium magnetization direction in the ferromagnetic layer [41]. This allows for the solution of the longitudinal spin accumulation problem in the usual manner developed for spin-dependent transport in current-perpendicular-to-plane giant magnetoresistive structures. Then the transverse problem can be solved in terms of a perturbation approach.

To understand how the separation of spin accumulation into transverse and longitudinal components permits solution of this problem, let us consider the spin torque exerted at a single FM/NM interface. If the magnetization is uniform, there is a net background "sea" of accumulated longitudinal spin $u_0$ (having units of density) at the interface, which can be calculated by straightforward methods for spin-dependent transport when current is flowing perpendicular to the plane of the multilayer structure [47]. If, however, the magnetization deviates from the uniform state by virtue of there being an additional spatially varying "transverse" component $\vec{M}_\perp(\vec{r})$, such that $\vec{M}(\vec{r}) = \vec{M}_0 + \vec{M}_\perp(\vec{r})$, where $\vec{M}_0 \cdot \vec{M}_\perp(\vec{r}) = 0$, then there is also an additional transverse component of the spin accumulation $\vec{u}_\perp(\vec{r})$, which can be written in reciprocal space as $\vec{\tilde{u}}_\perp(\vec{k}) = G(\vec{k})\vec{\tilde{M}}(\vec{k})$ [41] where $G(\vec{k})$ contains the details of the transverse spin diffusion process. In real space, the transverse spin accumulation may be written as $\vec{u}_\perp(\vec{r}) = F(\vec{M}(\vec{r}))$, where $F$ is the commensurate convolution operator. The resultant spin torque surface density is therefore

$$\vec{N}(\vec{r}) = \hbar w_0(\vec{u}_\perp(\vec{r}) - u_0\vec{m}_\perp(\vec{r})), \tag{13}$$

where $w_0$ is the effective interfacial scattering velocity for the spin transfer process, and $\vec{m}_\perp(\vec{r}) \doteq \vec{M}_\perp(\vec{r})/M_0$. Fig. 7 shows a simple schematic of how we can understand the two terms in Eq. (13) in the context of the elementary spin reflection processes on the NM side of the NM/FM interface. While the second term in Eq. (13) is analogous to the usual Slonczewski spin torque due to a background of non-collinear (but uniform) spin accumulation, the first

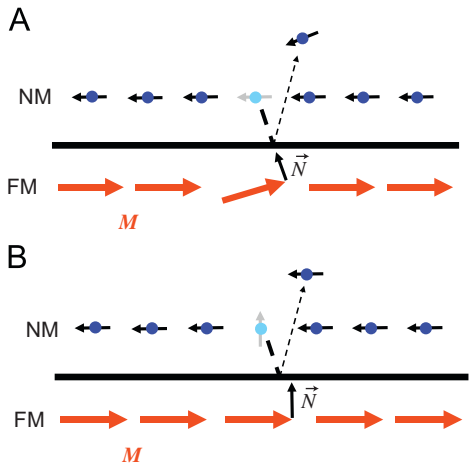


Fig. 7. Schematic of contributions to spin torque due to non-uniform magnetization and non-uniform spin accumulation. (A) Spin from the longitudinal "sea" of accumulated spins scatters from a region of non-uniform magnetization, generating a torque that increases non-uniformity in both the magnetization and the spin accumulation. This is described quantitatively by the second term in Eq. (13). (B) Non-uniform spin accumulation with non-zero transverse angular momentum scatters from uniform magnetization, generating a torque to increase the non-uniformity of the magnetization. This process is described quantitatively by the first term in Eq. (13).

term is the new contribution to the spin torque due to non-uniform "excess" spin accumulation.

Note that for several of the existent theories [41,42], spin waves of a particular wavenumber become unstable at sufficiently high currents, but that the wavenumber of the unstable spin waves is not a function of the contact dimension. (Indeed, these theories actually ignore the contact dimensions, in order to make the problem tractable.) This is in clear distinction to the case of spin-torque-induced oscillations in a point contact with a magnetic trilayer structure without lateral spin diffusion, where the characteristic length that sets the spin wave wavenumber is the contact size [13]. Instead, the spin diffusion length in proximity to the ferromagnetic layer sets the characteristic length scale for the problem with lateral spin diffusion. Presumably, in a real spin torque nano-oscillator, there is a competition between the contact dimension and the spin diffusion length as the dominant length scale of importance.

Brataas et al. [48] have calculated the threshold current for a standard five-layer structure with a putative nanopillar geometry, utilizing a theory that includes the effects of lateral spin diffusion. However, the lateral length scale of the nanopillar is again ignored as a simplifying assumption, thereby neglecting any boundary conditions that might affect the resultant dynamics. An alternative approach by Xi et al. [45] is to assume that the point contact is infinitesimally narrow in lateral extent and that the excited film is of a finite radius, centered at the contact, thereby ignoring any self-consistent contribution of lateral spin diffusion to the mode structure. In both cases what is lacking is an understanding of the competition between contact size and lateral spin diffusion in establishing the spatial profile of the excited mode.

Adam et al. [43] demonstrated a numerical proof-of-concept model for the integration of spin diffusion effects into micromagnetic simulations. Using this model, the authors predict that the dc resistance of the structure is reduced at the onset of microwave dynamics, and that chaotic dynamics ensue at sufficiently large dc currents in the absence of any applied magnetic field. However, an unrealistic geometry was used for the spin torque structure (a quasi-one-dimensional active layer), and the dipole (demagnetizing) fields were ignored. Indeed, the authors themselves admit that the model lacks the spatial resolution and physical realism to be considered quantitatively predictive.

The separation of spin accumulation into longitudinal and transverse components is strictly valid only in the limit of small deviations of the magnetization from uniform orientation; errors accumulate when the non-uniformities of the magnetization are no longer small. A consistent solution for the spin accumulation with arbitrarily inhomogeneous magnetization would be particularly helpful for a quantitative understanding how this "self" torque affects mode structure in spin torque nano-oscillators. Not only are there nonlinearities in the magnetic response, but there are also nonlinearities of the spin accumulation in response to large amplitude magnetization dynamics that must also be taken into account.

## 6. Conclusion

Spin torque nano-oscillators are novel microwave components that show promise for future spintronic applications. Such oscillators based upon point-contact geometry exhibit the narrowest room temperature linewidths, and are capable of mutual phase locking between two oscillators due to spin wave coupling in a shared active magnetic layer. While strides have been made to explain the coarse properties of spin torque nano-oscillators, and to improve the practicality of such devices, greater understanding of the detailed physics underlying spin torque dynamics is essential if progress towards practical applications is to continue. We have outlined some of the outstanding unanswered questions associated with the details of spin torque nano-oscillators in point contacts, though we have also endeavored to show that these so-called "details," which are often ignored or oversimplified in theoretical treatments, actually have great importance in affecting measured properties.

We do not consider this list of questions to be exhaustive. Of course, there are also many engineering issue that would also need to be addressed before spin torque oscillators will ever have practical utility. For example, there is the question of impedance matching between the spin torque nano-oscillator and an interconnecting waveguide, or how to array such devices for increased output power and stability [2,49]. There is also the possibility of using magnetic tunnel junctions to greatly increase the emitted microwave power [50], though whether magnetic tunnel junctions are compatible with point-contact geometry remains an open question. Nevertheless, it is expected that continued development of new magnetic material systems and spin torque geometries will fuel further improvements in device performance, and that enhanced understanding of the numerous "details" that affect spin torque dynamics in point contact structures will guide the development of such future materials and geometries.

## Acknowledgements

We gratefully acknowledge the very helpful discussions with Mark Hoefer, Mark Stiles, Steve Russek, and Andrei Slavin. We also appreciate the many useful editorial suggestions provided by Dan Ralph and Mark Stiles.

## References

[1] W.H. Rippard, M.R. Pufall, S. Kaka, et al., Phys. Rev. Lett. 92 (2004) 027201.
[2] S. Kaka, M.R. Pufall, W.H. Rippard, et al., Nature 437 (2005) 389.

[3] M.R. Pufall, W.H. Rippard, S. Kaka, et al., Appl. Phys. Lett. 86 (2005) 082506;
W.H. Rippard, M.R. Pufall, S. Kaka, et al., Phys. Rev. Lett. 95 (2005) 067203.
[4] W.H. Rippard, M.R. Pufall, S. Kaka, et al., Phys. Rev. B 70 (2004) 100406.
[5] J.C. Sankey, P.M. Braganca, A.G.F. Garcia, et al., Phys. Rev. Lett. 96 (2006) 227601;
G.D. Fuchs, J.C. Sankey, V.S. Pribiag, et al., Appl. Phys. Lett. 91 (2007) 062507;
A.A. Tulapurkar, Y. Suzuki, A. Fukushima, et al., Nature 438 (2005) 339.
[6] W.H. Rippard, M.R. Pufall, S.E. Russek, Phys. Rev. B 74 (2006) 224409.
[7] M.R. Pufall, W.H. Rippard, M.L. Schneider, et al., Phys. Rev. B 75 (2007) 140404.
[8] M.R. Pufall, W.H. Rippard, M.L. Schneider, et al., Phys. Rev. B 75 (14) (2007) 140404;
O. Boulle, V. Cros, J. Grollier, et al., Nat. Phys. 3 (2007) 492;
D. Houssameddine, U. Ebels, B. Delaet, et al., Nat. Mater. 6 (2007) 447.
[9] V.S. Pribiag, I.N. Krivorotov, G.D. Fuchs, et al., Nat. Phys. 3 (2007) 498.
[10] V. Novosad, F.Y. Fradin, P.E. Roy, et al., Phys. Rev. B 72 (2005) 024455.
[11] F.B. Mancoff, N.D. Rizzo, B.N. Engel, et al., Nature 437 (2005) 393.
[12] M.R. Pufall, W.H. Rippard, S.E. Russek, et al., Phys. Rev. Lett. 97 (8) (2006) 087206.
[13] J.C. Slonczewski, J. Magn. Magn. Mater. 195 (1999) L261.
[14] S.I. Kiselev, J.C. Sankey, I.N. Krivorotov, et al., Nature 425 (2003) 380.
[15] I.N. Krivorotov, D.V. Berkov, N.L. Gorn, et al., Phys. Rev. B 76 (2007) 024418.
[16] J.C. Sankey, I.N. Krivorotov, S.I. Kiselev, et al., Phys. Rev. B 72 (2005) 224427.
[17] S.I. Kiselev, J.C. Sankey, I.N. Krivorotov, et al., Phys. Rev. B 72 (6) (2005) 064430.
[18] A.H. Morrish, The Physical Principles of Magnetism, IEEE Press, New York, 2001.
[19] H. Suhl, J. Phys. Chem. Solids 1 (1957) 209.
[20] T. Gerrits, P. Krivosik, M.L. Schneider, et al., Phys. Rev. Lett. 98 (20) (2007) 207602;
G. de Loubens, V.V. Naletov, O. Klein, Phys. Rev. B 71 (18) (2005) 180411.
[21] D.D. Stancil, Theory of Magnetostatic Waves, Springer, New York, 1993.
[22] H. Xia, P. Kabos, H.Y. Zhang, et al., Phys. Rev. Lett. 81 (2) (1998) 449;
M. Bauer, O. Büttner, S.O. Demokritov, et al., Phys. Rev. Lett. 81 (17) (1998) 3769.
[23] M. A. Hoefer, University of Colorado, Boulder, 2006.
[24] M.R. Pufall, W.H. Rippard, S.E. Russek, et al., Phys. Rev. Lett. 97 (2006) 087206.
[25] A. Slavin, V. Tiberkevich, Phys. Rev. Lett. 95 (23) (2005) 237201.
[26] M.A. Hoefer, M.J. Ablowitz, B. Ilan, et al., Phys. Rev. Lett. 95 (2005) 267206.
[27] I.S. Aranson, L. Kramer, Rev. Mod. Phys. 74 (2002) 99.
[28] A. Hasegawa, Optical Solitons in Fibers, second ed., Springer, Berlin, 1990;
M. Chen, J.M. Nash, C.E. Patton, J. Appl. Phys. 73 (8) (1993) 3906.
[29] M.J. Lighthill, J. Inst. Math. Appl. 1 (1965) 269;
B.A. Kalinikos, N.G. Kovshikov, A.N. Slavin, J. Appl. Phys. 67 (9) (1990) 5633.
[30] V. Tiberkevich, A. Slavin, Phys. Rev. B 75 (1) (2007) 014440.
[31] V. Kambersky, C.E. Patton, Phys. Rev. B 11 (7) (1975) 2668.
[32] K. Gilmore, Y.U. Idzerda, M.D. Stiles, Phys. Rev. Lett. 99 (2) (2007) 027204.
[33] G. Consolo, B. Azzerboni, G. Gerhart, et al., Phys. Rev. B 76 (2007) 144410.
[34] T.J. Silva, M. A. Hoefer, unpublished, 2007.
[35] M.J. Donahue, D.G. Porter, National Inst. Std. Tech. NISTIR, 1999, 6376.
[36] J.P. Park, P. Eames, D.M. Engebretson, et al., Phys. Rev. Lett. 89 (2002) 277201;
J. Jorzick, S.O. Demokritov, B. Hillebrands, et al., Phys. Rev. Lett. 88 (2002) 047204;
R.D. McMichael, B.B. Maranville, Phys. Rev. B 74 (2006) 024424.
[37] J.-V. Kim, V. Tiberkevich, A.N. Slavin, arXiv:cond-mat/0703317v2, 2007.
[38] A.N. Slavin, V.S. Tiberkevich, Phys. Rev. B 74 (2006) 104401.
[39] E. Martinez, L. Lopez-Diaz, L. Torres, et al., J. Phys. D 40 (2007) 942.
[40] P.E. Wigen, R.D. McMichael, C. Jayaprakash, J. Magn. Magn. Mater. 84 (3) (1990) 237.
[41] M.D. Stiles, J. Xiao, A. Zangwill, Phys. Rev. B 69 (2004) 054408.
[42] M.L. Polianski, P.W. Brouwer, Phys. Rev. Lett. 92 (2004).
[43] S. Adam, M.L. Polianski, P.W. Brouwer, Phys. Rev. B 73 (2006) 024425.
[44] A. Brataas, Y. Tserkovnyak, G.E.W. Bauer, Phys. Rev. B 73 (2006).
[45] H.W. Xi, Y.Z. Yang, O.Y. Jun, et al., Phys. Rev. B 75 (2007).
[46] Y. Ji, C.L. Chien, M.D. Stiles, Phys. Rev. Lett. 90 (10) (2003) 106601;
B. Ozyilmaz, A.D. Kent, J.Z. Sun, et al., Phys. Rev. Lett. 93 (2004) 176604;
B. Ozyilmaz, A.D. Kent, Appl. Phys. Lett. 88 (16) (2006) 162506.
[47] T. Valet, A. Fert, Phys. Rev. B 48 (10) (1993) 7099.
[48] A. Brataas, Y. Tserkovnyak, G.E.W. Bauer, Phys. Rev. B 73 (1) (2006) 014408.
[49] J. Grollier, V. Cros, A. Fert, Phys. Rev. B 73 (2006) 060409.
[50] Appl. Phys. Lett. 85 (2004) 1205;
J.C. Slonczewski, Phys. Rev. B 71 (2005) 024411;
G.D. Fuchs, J.A. Katine, S.I. Kiselev, et al., Phys. Rev. Lett. 96 (2006) 186603;
S. Petit, C. Baraduc, C. Thirion, et al., Phys. Rev. Lett. 98 (2007) 077203.